JOURNAL OF THERMOPHYSICS AND HEAT TRANSFER
Vol. 11, No. 2, April–June 1997

# Experimental Thermal Contact Conductance of Electronic Modules

M. A. Lambert*
*San Jose State University, San Jose, California 95192-0087*
and
I. G. Cavenall† and L. S. Fletcher‡
*Texas A&M University, College Station, Texas 77843-3123*

**The Standard Electronic Module, format E, (SEM-E) is extensively employed in navigation, control, tracking, guidance, and communications electronics. Thermal resistance of the junction between the guide rib of the SEM-E frame and the liquid-cooled chassis card rail to which the module is clamped is a principal contributor to overall thermal resistance in the heat rejection path. High resistance causes excessive operating temperatures and failure rates. The currently used configuration employs anodic coatings on contact surfaces and segmented wedge clamps to secure modules to the chassis. In the present investigation, the thermal performance of alternative configurations utilizing nickel and silver platings instead of the anodic coating on card rails and pneumatic bladder clamps instead of wedge clamps is experimentally determined. These results are compared to previously obtained results for the baseline condition. Results indicate that nickel and silver platings and bladder clamps provide no enhancement in performance in an ambient air environment (in which surface vessels and submarines operate) compared to anodic coatings and wedge clamps. In a vacuum environment (approximating operational surroundings for high-altitude aircraft and spacecraft), nickel plating increases junction thermal resistance by 300%, silver plating reduces resistance by 25–33%, and bladder clamps decrease resistance by 25–40%.**

## I. Introduction

A RECURRENT problem in the operation of high-power electronics is heat dissipation. Large-scale computer architecture often utilizes modular components at the system level to facilitate assembly, maintenance, adaptability, and expansion. In particular, the Standard Electronic Module (SEM) is widely incorporated in military electronics for navigation, sensing, guidance, and communications for surfaces vessels, submarines, and aircraft. Great attention has been paid to most aspects of minimizing thermal resistance between the electronics on each module and the liquid-cooled chassis to which the modules are mounted. For example, the dielectric material in SEM circuit boards is a ceramic (alumina, $Al_2O_3$), the thermal conductivity of which is roughly an order of magnitude greater than the thermal conductivity of more commonly used organic polymers. However, junction thermal resistance between the module guide rib and the chassis card rail (Fig. 1) is substantial and is the greatest contributor to thermal resistance in the heat rejection path.

A wedge clamp is used to press the guide rib against the card rail to facilitate thermal conductance. However, such clamps generate nonuniform pressure over the apparent contact interface, resulting in macroscopic gaps between the surfaces and associated high thermal resistance. Additionally, format E modules (SEM-E), specified for an increasingly greater proportion of modules, and card rails are made of aluminum alloys that are anodized to enhance corrosion resistance. Anodic coatings are thermal insulators and quite hard. High hardness limits plastic deformation under load of the microscopic surface irregularities characteristic of rough surfaces (produced by machining, casting, or extruding), thus limiting the real contact area of the microscopic contact spots (heat conduction paths).

The thermal resistance of the guide rib/card rail junction can be reduced by a number of methods: making the contact pres-

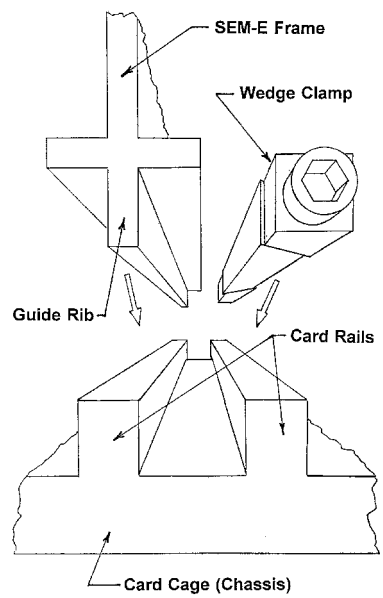


**Fig. 1 Junction between SEM-E frame guide rib and chassis card rail, showing a wedge clamp.**

Presented as Paper 96-1825 at the AIAA 31st Thermophysics Conference, New Orleans, LA, June 17–20, 1996; received June 26, 1996; revision received Dec. 27, 1996; accepted for publication Dec. 30, 1996. 

*Assistant Professor, Department of Mechanical Engineering. Member AIAA.

†Graduate Research Assistant, Department of Mechanical Engineering. Student Member AIAA.

‡Thomas A. Dietz Professor, Department of Mechanical Engineering. Fellow AIAA.

sure more uniform to eliminate macroscopic gaps; applying softer, more thermally conductive coatings or interstitial materials; increasing apparent contact pressure; augmenting apparent contact area; and specifying smoother, flatter surfaces. For SEM-E applications, apparent contact pressure cannot be significantly increased without increased risk of mechanical failure of wedge clamps, and apparent contact area cannot be augmented without costly system redesign and retrofitting. Specifications for surface roughness and flatness approach the limits of commercial high-production extrusion and milling operations. Hence, the only avenues remaining by which SEM-E joint conductance may be enhanced are improved coatings and alternative clamping devices that provide more uniform contact pressure. Both methods provide greater true contact area.

Lambert and Fletcher[1] surmised that metallic coatings are superior to thermally conductive greases, thin metallic foils and elastomeric films, and low-melting temperature eutectic alloys with regard to durability, ease of application, and potential contact conductance enhancement. Lambert and Fletcher[1] determined that of all the metallic elements, silver possessed the optimal combination of high conductivity, relatively low hardness, corrosion resistance, ease of application, and cost effectiveness. Of the methods available for applying metallic coatings, Lambert and Fletcher[2] experimentally demonstrated that silver electroplatings provide greater conductance enhancement and corrosion resistance than vapor deposited and flame-sprayed silver coatings.

A segmented wedge clamp contacts only a portion of the guide rib, which is relatively thin and compliant. Thus, the guide rib bends, contacting the card rail only near where the wedge clamp segments contact the guide rib, leaving macroscopic gaps at other locations along the interface between the guide rib and card rail. A bladder clamp, which provides uniform contact pressure over the entire guide rib, can eliminate or reduce macroscopic gaps between the guide rib and card rail.

## II. Experimental Program

This investigation is directed toward experimentally measuring the junction thermal conductance and related parameters for baseline (presently used) and alternative coatings and clamping devices for SEM-E guide ribs and card rails. The test facility, coatings, clamps, procedure, and data analysis are described next.

### A. Test Facility

Thermal tests were performed using the facility illustrated in Fig. 2. It consists of a liquid-cooled chassis card rail, SEM-E frame, wedge clamp, and a radiation shield/enclosure to simulate the adjacent modules. Two 50-W silicone pad heaters are mounted on either side of the SEM-E frame to simulate the electronics. Seventeen K-type (chromel–alumel) 36 AWG thermocouples (T/Cs) are mounted to the SEM-E frame (9 T/Cs), card rail (6 T/Cs), and radiation shield/enclosure (2 T/Cs).

A small dc motor/gearbox is used to vary torque on the wedge clamp screw. Generated torque is calibrated with respect to electrical current supplied to the motor. For tests involving bladder clamps instead of wedge clamps, the motor/gearbox is replaced by a tube supplying nitrogen gas at manually regulated pressure.

Thermocouple temperatures are recorded and heater power and current to the motor (and, in turn, wedge clamp torque) are automatically controlled by a 486DX/66MHz computer. The control and data acquisition software provides real time graphical displays of temperature profile, power dissipation, torque, and junction thermal conductance.

All tests were performed with SEM-E frames that were cut in half along the longitudinal axis. Thus, there was only one guide rib/card rail junction instead of two for a complete

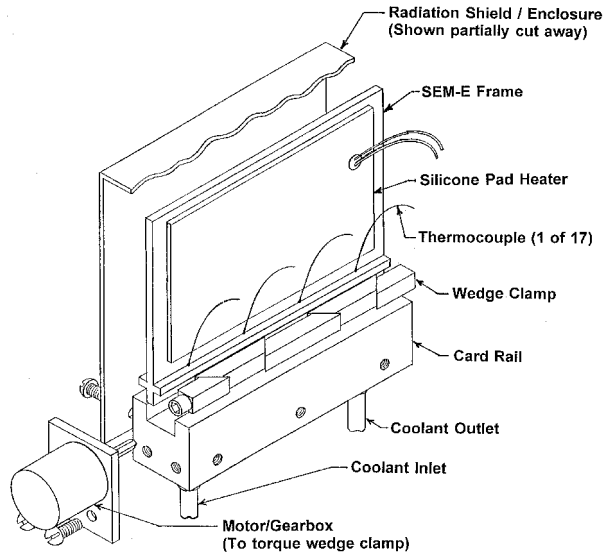


**Fig. 2 Schematic view of the experimental thermal test facility for a full SEM-E frame. A half SEM-E frame was tested to take advantage of symmetry.**

SEM-E frame. This was done to take advantage of the symmetry of the SEM-E, which permits testing of a half frame in lieu of a full frame.

The facility is housed in a vacuum chamber that may be used to reduce convective heat losses and gas gap conductance to negligible amounts. This allows the contribution of thermal contact (solid spot) conductance to overall junction thermal conductance to be determined. Testing under vacuum simulates a high altitude or space environment for which gas gap conductance may be severely reduced or nonexistent.

### B. Test Matrix

The test matrix variables are operating environment, power, clamp torque or bladder pressure, and card rail coating. Two environments were used, air at atmospheric pressure (336 ft above sea level) and moderate relative humidity (approximately 60%) and a vacuum of 300 mtorr or less. The atmospheric environment tests are comparable to SEM-E use in surface vessels and submarines; whereas the vacuum environment simulates the environment for high-altitude aircraft or spacecraft.

Total power supplied to the two pad heaters was increased geometrically (doubled each increment) from 5 to 80 W (i.e., 5, 10, 20, 40, and 80 W) for tests in air and from 5 to 40 W for tests in vacuum. SEM-Es currently operate at 10–40 W (5–20 W per circuit board), though higher power modules are envisioned for future applications. As previously stated, all testing was performed on half SEM-E frames instead of full SEM-E frames to take advantage of symmetry. Thus, all power levels used in testing would be doubled to correspond to equivalent conditions for a complete SEM-E in service.

The clamping devices are of two types: 1) the currently utilized five-segment wedge clamp and 2) the new pneumatic bladder clamp. Wedge clamp torque was increased from 0.56 to 1.58 N-m (5–14 lbf-in.) in 0.34 N-m (3 lbf-in.) steps. A wedge clamp torque of 0.90 N-m (8 lbf-in.) is specified in maintenance manuals. Bladder clamp pressure was increased from 689 kPa (100 psig) to 1378 kPa (200 psig) in 345 kPa (50 psig) steps. The contact pressure generated by the five-segment wedge clamps is on the order of 2504 kPa per N-m (41 psig per lbf-in.). Therefore, for the maximum applied torque of 1.58 N-m (14 lbf-in.), the corresponding contact pressure is 3958 kPa (574 psig).

The card rail coatings are type II (soft coat) anodization (currently specified for aluminum alloy 6101-T6 SEM-E format frames), electroless nickel plating (widely used for cor-

rosion prevention and currently used on copper SEM-D format frames), and electroplated silver as recommended by Lambert and Fletcher.[2]

All tests were performed in triplicate. That is, three SEM-E frames, each paired with a different five-piece wedge clamp or bladder clamp, were tested in conjunction with each of three card rails (one anodized, the second electroless nickel plated, and the third silver electroplated). This was done to ensure repeatable, truly representative results.

### C. Card Rail Coatings

The SEM-E frames are presently coated by a type III (hard coat, chilled processing) anodization, and the card rail chassis is coated by a type II (soft coat, room temperature processing) anodization. To maintain electrical isolation of each module from the chassis, only the anodic (nonconductive) coating on either the guide rib or card rail, but not on both, may be replaced by a metallic coating for conductance enhancement. Since the guide ribs comprise only a small portion of the frames, to eliminate the need for two coating processes (metal plating on the guide rib and anodization on the remainder of the SEM frame) it was deemed more appropriate to plate the chassis card rails instead.

Anodized SEM-E aluminum alloy 6101-T6 (although aluminum alloy 6061-T6 is sometimes substituted) frames were obtained from the manufacturer. The aluminum alloy A356-T61 card rails were coated (anodized, electroless nickel plated, and silver electroplated) at Texas A&M University using techniques described next.

The first aluminum card rail was anodized to a thickness of 18 $\mu$m (0.7 mil) in room temperature (25°C), 15-wt% sulfuric acid employing a process described by Darrow,[3] which yielded a type II (soft) coating. A second card rail was precoated with a zincate solution formulated by Dini and Johnson[4] to remove oxidized aluminum, then overplated with electroless nickel to a thickness of approximately 76 $\mu$m (3.0 mil) using a solution developed by Maclean and Karten[5] and a procedure outlined by Krieg.[6] A third card rail was given the same zincate precoating, then silver electroplated in two steps (an initial strike thin plating followed by a thick main plating) to a thickness of approximately 500 $\mu$m (20 mil), and finally ground to a thickness of approximately 250 $\mu$m (10 mil). Blair[7] provided the formula for the strike plating. Sora and Bollhalder[8] reported the formula for the main silver plating.

### D. Bladder Clamps

The bladder clamps are cylindrical and are made of latex rubber. The outside and inside diameters of the bladder are 4.76 mm (0.1875 in.) and 1.59 mm (0.0625 in.), respectively, and the length is 15 cm (6 in.). These dimensions match those of the presently used wedge clamps. Each bladder clamp is housed in a three-sided C-channel to constrain expansion of the bladder when pressurized. The open fourth side of the C-channel faces the guide rib to allow the expanding bladder to press the guide rib against the card rail.

### E. Experimental Procedure

Each test is begun by attaching one of three card rails (either anodized or nickel plated or silver plated) to the motor/gearbox (for tightening the wedge clamp screws) or the nitrogen supply tube (for pressurizing the bladder clamps). The card rail is also attached to the coolant hoses in the vacuum chamber and cleaned with acetone. Next, one of three (for triplicate testing) identical half SEM-E frames and a wedge clamp or bladder clamp are cleaned with acetone and inserted into the card rail slot. The heat shield/enclosure is secured around the SEM-E half-frame. The heater and motor power leads and thermocouples (bonded to the card rail, SEM-E frame, and enclosure) are connected and checked. The vacuum bell is lowered (and evacuated for vacuum tests), and the coolant valve is opened.

The desired test matrix is entered into the control and data acquisition program and it is executed. When all desired data have been gathered in vacuum, the chamber is vented and the test is repeated for an ambient environment.

### F. Data and Error Analysis

Data recorded include heater power, clamp torque, or bladder pressure, and the readings from 17 thermocouples mounted to the card rail (6), SEM-E frame (9), and the heat shield/enclosure (2), plus two additional thermocouples for measuring environmental temperature. Temperature readings are utilized in calculating radiative and convective heat losses, junction thermal conductance and resistance, mean junction temperature, temperature drop across the junction, and maximum SEM-E frame temperature.

Torque is known to an accuracy of 0.057 N-m (0.5 lbf-in.), bladder pressure to 14 kPa (2 psig), and heater power to 0.5 W. Thermocouple temperatures are known to within 1.1 K (2.0°F) and relevant dimensions are known to within 0.1 mm (0.004 in.). Using the method of Kline and McClintock[9] the overall uncertainty ranges from 13% at the lowest heater power to 7% at the highest power. The maximum difference between any individual result (temperature, conductance, or resistance) and its corresponding average for the triplicate tests was less than 10% for wedge clamps tests and 15% for bladder clamp tests.

## III. Results and Discussion

The experimental thermal test results of the baseline configuration (type II anodized card rail and five-piece wedge clamp) are compared with the results for alternative coatings (electroless nickel and silver on the card rail) and new bladder clamps.

Each of the data represented in the figures and tables that are described next represents the average of the three values from the triplicate tests (three different SEM-E frames and wedge or bladder clamps) for the particular test condition (i.e., environment, torque, power, card rail coating). As mentioned earlier, all tests were performed with half SEM-E frames (with one guide rib) instead of full frames (with two guide ribs) to take advantage of the bilateral symmetry of SEM-E frames. Power levels shown in the figures discussed next are for tests of half SEM-E frames. These power values would be doubled to predict the performance of full frames.

### A. Baseline: Anodized Card Rail and Wedge Clamp

Figures 3a–3e depict the results of thermal tests of the baseline SEM-E configuration that utilizes a type II anodized card rail and five-piece wedge clamps. These results, also listed in Tables 1–5, were previously reported by Lambert et al.,[10] and are included here for comparison to new results for alternative coatings and clamps. Figure 3a and Table 1 show junction thermal conductance as a function of wedge clamp torque for several power levels. The conductance in air is approximately an order of magnitude greater than the conductance in vacuum. This is because most of the heat is transported across the junction by conduction through air gaps. Also, for air tests conductance increases moderately with torque and power, whereas for vacuum tests conductance increases markedly with both power and torque. Because the contribution of contact conductance to junction conductance is small, the marked increase in contact conductance with increasing torque has a minimal effect on junction conductance.

Junction thermal resistance as a function of both torque and power is plotted in Fig. 3b and listed in Table 2. Thermal resistance is the reciprocal of thermal conductance, without normalization with respect to contact area, as shown by the units on the figure axes. Thus, the same observations noted for junction conductance also apply for junction resistance. The mean resistance in an air environment is 0.24 K/W.

Mean junction temperature is graphed in Fig. 3c and listed in Table 3 as a function of torque for several power levels.

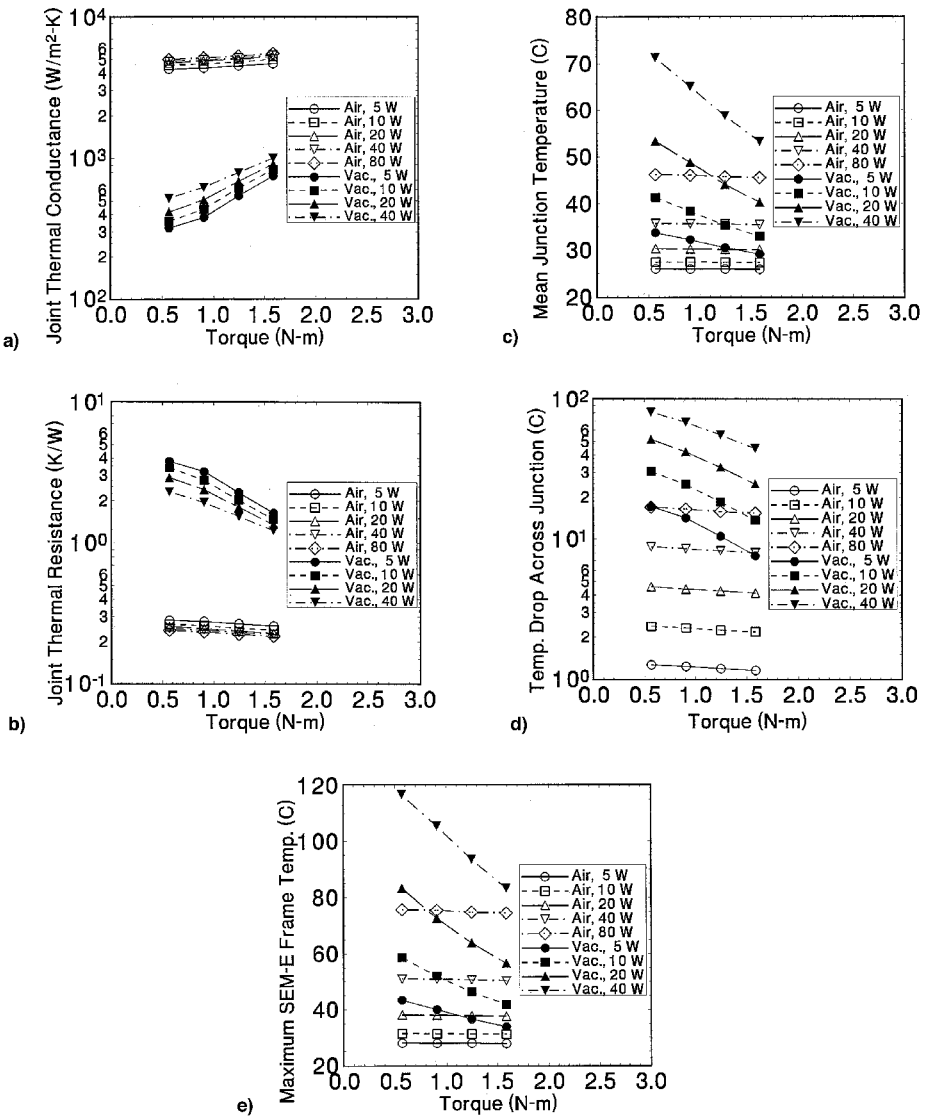


**Fig. 3 Thermal test results: a) junction thermal conductance, b) junction thermal resistance, c) mean junction temperature, d) temperature drop across junction, and e) centerline (maximum) SEM-E frame temperature for triplicate tests of anodized (type III) SEM-E frames pressed against an anodized (type II) card rail by five segment wedge clamps in air and vacuum environments.**

The maximum permissible junction temperature is 60°C. For the coolant temperature (25°C) utilized in the present half SEM-E tests, performance in an air environment is within specifications for power levels up to rated power, that is, up to 20 W for a half SEM-E (40 W for a full SEM-E). The same observations hold for tests in vacuum, except that for the highest power, 40 W for a half SEM-E (80 W for full SEM-E), the torque must be greater than 1.13 N-m (10 lbf-in.) to maintain a mean junction temperature below 60°C.

Figure 3d and Table 4 show the temperature drop across the guide rib/card rail junction as a function of the torque and power. For tests in both air and vacuum, the temperature drop increases proportionately to power. That is, geometric increases (i.e., doubled with each increment) in power result in nearly doubled temperature drops. For vacuum conditions, note the very large temperature drops for high-power tests.

Maximum (centerline) temperature for the half SEM-E frames for the range of applied torque and consumed power is presented in Fig. 3e and Table 5. Centerline temperature is measured at the top edge of the half SEM-E frames, which corresponds to the line of symmetry of full SEM-E frames. The maximum allowable device temperature is 85°C. The corresponding maximum SEM-E frame temperature must be considerably lower because of the added thermal resistance of solder bonds between devices and the circuit board, the circuit board itself, and resistance at the interface between the circuit board and the SEM-E frame. For the coolant temperature (25°C) employed in the present tests, the performance in air is within acceptable limits for power levels up to the rated power, that is, up to 20 W for a half SEM-E (40 W for a full SEM-E). However, an overload of 80 W (160 W for a full SEM-E) will most likely result in unacceptably high maximum device temperatures. The performance in vacuum is less than 85°C for power levels up to 10 W for a half SEM-E (20 W for a full SEM-E). For a rated power of 20 W for a half SEM-E (40 W for a full SEM-E), torque must be near the upper limit tested to maintain the maximum device temperature below 85°C. For the overload power, 40 W for a half SEM-E (80 W for a full SEM-E), the maximum device temperature will exceed 85°C for all torque levels.

### B. Alternative (Metallic) Card Rail Coatings

#### *1. Electroless Nickel Plating*

Tables 1–5 list the results of thermal tests of the electroless nickel-plated card rail and wedge clamps. In air, the junction thermal conductance (Table 1) of the anodized SEM-E frame to the nickel-plated card rail (anodized-to-nickel) is approxi-

**Table 1 Junction thermal conductance, W/m²-K**

| | Anodic rail/wedge clamp torque, N-m/lbf-in. | | | | Silver rail/wedge clamp torque, N-m/lbf-in. | | | | Nickel rail/wedge clamp torque, N-m/lbf-in. | | | | Anodic rail/bladder pressure, MPa/psig | | | Silver rail/bladder pressure, MPa/psig | | |
|---|---|---|---|---|---|---|---|---|---|---|---|---|---|---|---|---|---|---|
| Power, | 0.56 | 0.90 | 1.24 | 1.58 | 0.56 | 0.90 | 1.24 | 1.58 | 0.56 | 0.90 | 1.24 | 1.58 | 0.689 | 1.034 | 1.378 | 0.689 | 1.034 | 1.378 |
| W | 5 | 8 | 11 | 14 | 5 | 8 | 11 | 14 | 5 | 8 | 11 | 14 | 100 | 150 | 200 | 100 | 150 | 200 |
| Air | | | | | | | | | | | | | | | | | | |
| 5 | 4261 | 4341 | 4507 | 4664 | 3525 | 3813 | 3932 | 4073 | 1024 | 1061 | 1092 | 1150 | 2439 | 2728 | 2750 | 2180 | 2362 | 2562 |
| 10 | 4550 | 4650 | 4774 | 5024 | 3918 | 4122 | 4318 | 4439 | 1123 | 1163 | 1201 | 1257 | 2533 | 2888 | 2954 | 2296 | 2620 | 2783 |
| 20 | 4718 | 4885 | 5029 | 5246 | 4159 | 4336 | 4558 | 4759 | 1205 | 1244 | 1291 | 1345 | 2631 | 2989 | 3069 | 2333 | 2685 | 2857 |
| 40 | 4854 | 4985 | 5128 | 5351 | 4272 | 4494 | 4746 | 4945 | 1284 | 1298 | 1371 | 1422 | 2722 | 3075 | 3113 | 2406 | 2739 | 2923 |
| 80 | 5007 | 5139 | 5301 | 5517 | 4327 | 4562 | 4804 | 5024 | 1375 | 1413 | 1461 | 1521 | 2715 | 3121 | 3148 | 2501 | 2776 | 3007 |
| Vacuum | | | | | | | | | | | | | | | | | | |
| 5 | 319 | 380 | 542 | 750 | 508 | 670 | 843 | 1016 | 219 | 244 | 283 | 346 | 282 | 407 | 641 | 376 | 555 | 648 |
| 10 | 357 | 436 | 614 | 832 | 563 | 740 | 926 | 1116 | 237 | 268 | 319 | 385 | 288 | 440 | 721 | 416 | 653 | 749 |
| 20 | 417 | 508 | 686 | 908 | 646 | 829 | 1011 | 1215 | 259 | 305 | 358 | 426 | 298 | 463 | 764 | 435 | 686 | 800 |
| 40 | 521 | 623 | 792 | 1001 | 770 | 950 | 1130 | 1329 | 326 | 364 | 416 | 483 | 334 | 488 | 796 | 488 | 717 | 851 |

**Table 2 Junction thermal resistance, k/W**

| | Anodic rail/wedge clamp torque, N-m/lbf-in. | | | | Silver rail/wedge clamp torque, N-m/lbf-in. | | | | Nickel rail/wedge clamp torque, N-m/lbf-in. | | | | Anodic rail/bladder pressure, MPa/psig | | | Silver rail/bladder pressure, MPa/psig | | |
|---|---|---|---|---|---|---|---|---|---|---|---|---|---|---|---|---|---|---|
| Power, | 0.56 | 0.90 | 1.24 | 1.58 | 0.56 | 0.90 | 1.24 | 1.58 | 0.56 | 0.90 | 1.24 | 1.58 | 0.689 | 1.034 | 1.378 | 0.689 | 1.034 | 1.378 |
| W | 5 | 8 | 11 | 14 | 5 | 8 | 11 | 14 | 5 | 8 | 11 | 14 | 100 | 150 | 200 | 100 | 150 | 200 |
| Air | | | | | | | | | | | | | | | | | | |
| 5 | 0.282 | 0.277 | 0.267 | 0.258 | 0.341 | 0.316 | 0.306 | 0.296 | 1.17 | 1.13 | 1.11 | 1.05 | 0.495 | 0.440 | 0.430 | 0.554 | 0.517 | 0.472 |
| 10 | 0.264 | 0.259 | 0.248 | 0.241 | 0.308 | 0.292 | 0.279 | 0.271 | 1.07 | 1.04 | 1.00 | 0.957 | 0.475 | 0.416 | 0.408 | 0.525 | 0.463 | 0.435 |
| 20 | 0.255 | 0.246 | 0.238 | 0.229 | 0.290 | 0.278 | 0.264 | 0.253 | 1.00 | 0.969 | 0.932 | 0.894 | 0.457 | 0.402 | 0.393 | 0.516 | 0.452 | 0.423 |
| 40 | 0.248 | 0.241 | 0.233 | 0.225 | 0.282 | 0.268 | 0.254 | 0.244 | 0.940 | 0.914 | 0.878 | 0.846 | 0.442 | 0.391 | 0.387 | 0.501 | 0.444 | 0.414 |
| 80 | 0.240 | 0.234 | 0.225 | 0.218 | 0.279 | 0.264 | 0.251 | 0.240 | 0.877 | 0.852 | 0.824 | 0.791 | 0.443 | 0.385 | 0.383 | 0.481 | 0.430 | 0.402 |
| Vacuum | | | | | | | | | | | | | | | | | | |
| 5 | 3.78 | 3.19 | 2.28 | 1.64 | 2.43 | 1.82 | 1.44 | 1.19 | 5.60 | 5.01 | 4.34 | 3.54 | 4.37 | 2.99 | 1.89 | 3.35 | 2.05 | 1.86 |
| 10 | 3.38 | 2.78 | 2.02 | 1.48 | 2.18 | 1.64 | 1.30 | 1.08 | 5.19 | 4.56 | 3.82 | 3.17 | 4.28 | 2.77 | 1.67 | 3.05 | 1.87 | 1.60 |
| 20 | 2.89 | 2.39 | 1.80 | 1.35 | 1.89 | 1.46 | 1.19 | 0.992 | 4.69 | 3.98 | 3.41 | 2.86 | 4.14 | 2.63 | 1.58 | 2.92 | 1.79 | 1.50 |
| 40 | 2.31 | 2.31 | 1.55 | 1.23 | 1.58 | 1.27 | 1.07 | 0.906 | 3.71 | 3.34 | 2.93 | 2.52 | 3.67 | 2.50 | 1.51 | 2.59 | 1.69 | 1.41 |

**Table 3 Mean junction temperature, °C**

| | Anodic rail/wedge clamp torque, N-m/lbf-in. | | | | Silver rail/wedge clamp torque, N-m/lbf-in. | | | | Nickel rail/wedge clamp torque, N-m/lbf-in. | | | | Anodic rail/bladder pressure, MPa/psig | | | Silver rail/bladder pressure, MPa/psig | | |
|---|---|---|---|---|---|---|---|---|---|---|---|---|---|---|---|---|---|---|
| Power, | 0.56 | 0.90 | 1.24 | 1.58 | 0.56 | 0.90 | 1.24 | 1.58 | 0.56 | 0.90 | 1.24 | 1.58 | 0.689 | 1.034 | 1.378 | 0.689 | 1.034 | 1.378 |
| W | 5 | 8 | 11 | 14 | 5 | 8 | 11 | 14 | 5 | 8 | 11 | 14 | 100 | 150 | 200 | 100 | 150 | 200 |
| Air | | | | | | | | | | | | | | | | | | |
| 5 | 26.0 | 25.9 | 25.9 | 25.9 | 26.4 | 26.4 | 26.3 | 26.3 | 28.3 | 28.2 | 28.2 | 28.0 | 26.4 | 26.2 | 26.2 | 26.5 | 26.3 | 26.2 |
| 10 | 27.5 | 27.4 | 27.4 | 27.3 | 27.9 | 27.9 | 27.8 | 27.8 | 31.3 | 31.2 | 31.0 | 30.8 | 28.3 | 28.0 | 28.0 | 28.4 | 28.1 | 28.0 |
| 20 | 30.3 | 30.3 | 30.1 | 30.1 | 30.8 | 30.7 | 30.6 | 30.5 | 37.0 | 36.8 | 36.5 | 36.2 | 32.0 | 31.5 | 31.4 | 32.3 | 31.7 | 31.5 |
| 40 | 35.8 | 35.7 | 35.6 | 35.5 | 36.5 | 36.2 | 35.9 | 35.8 | 47.7 | 47.4 | 46.8 | 46.2 | 39.2 | 38.2 | 38.2 | 39.7 | 38.7 | 38.4 |
| 80 | 42.6 | 46.0 | 45.7 | 45.5 | 47.2 | 46.7 | 46.2 | 45.8 | 67.2 | 66.5 | 65.7 | 64.5 | 52.8 | 50.9 | 50.7 | 53.4 | 41.7 | 41.0 |
| Vacuum | | | | | | | | | | | | | | | | | | |
| 5 | 33.7 | 32.3 | 30.5 | 29.1 | 31.1 | 29.7 | 28.9 | 28.3 | 37.7 | 36.5 | 35.2 | 33.5 | 34.8 | 31.9 | 29.2 | 32.4 | 29.8 | 29.3 |
| 10 | 41.3 | 38.4 | 35.4 | 33.0 | 36.2 | 33.8 | 32.3 | 31.4 | 48.7 | 46.1 | 43.2 | 40.6 | 44.6 | 38.4 | 33.6 | 39.2 | 34.4 | 33.7 |
| 20 | 53.4 | 48.8 | 44.1 | 40.3 | 44.7 | 41.1 | 38.8 | 37.0 | 67.4 | 61.9 | 57.5 | 53.3 | 62.6 | 50.9 | 42.3 | 52.5 | 43.5 | 41.9 |
| 40 | 71.3 | 65.1 | 58.8 | 53.3 | 58.8 | 53.6 | 50.1 | 47.3 | 92.8 | 86.9 | 81.0 | 74.8 | 90.9 | 73.8 | 58.4 | 74.0 | 60.4 | 57.1 |

**Table 4 Temperature drop across junction, °C**

| | Anodic rail/wedge clamp torque, N-m/lbf-in. | | | | Silver rail/wedge clamp torque, N-m/lbf-in. | | | | Nickel rail/wedge clamp torque, N-m/lbf-in. | | | | Anodic rail/bladder pressure, MPa/psig | | | Silver rail/bladder pressure, MPa/psig | | |
|---|---|---|---|---|---|---|---|---|---|---|---|---|---|---|---|---|---|---|
| Power, | 0.56 | 0.90 | 1.24 | 1.58 | 0.56 | 0.90 | 1.24 | 1.58 | 0.56 | 0.90 | 1.24 | 1.58 | 0.689 | 1.034 | 1.378 | 0.689 | 1.034 | 1.378 |
| W | 5 | 8 | 11 | 14 | 5 | 8 | 11 | 14 | 5 | 8 | 11 | 14 | 100 | 150 | 200 | 100 | 150 | 200 |
| Air | | | | | | | | | | | | | | | | | | |
| 5 | 1.3 | 1.2 | 1.2 | 1.2 | 1.5 | 1.4 | 1.3 | 1.3 | 4.9 | 4.8 | 4.6 | 4.4 | 2.3 | 2.0 | 2.0 | 2.4 | 2.2 | 2.1 |
| 10 | 2.4 | 2.3 | 2.2 | 2.2 | 2.7 | 2.6 | 2.5 | 2.4 | 9.1 | 8.8 | 8.5 | 8.1 | 4.3 | 3.8 | 3.7 | 4.7 | 4.1 | 3.9 |
| 20 | 4.6 | 4.4 | 4.3 | 4.1 | 5.2 | 4.9 | 4.7 | 4.5 | 16.9 | 16.4 | 15.8 | 15.2 | 8.3 | 7.2 | 7.1 | 9.1 | 8.0 | 7.5 |
| 40 | 8.8 | 8.5 | 8.2 | 8.0 | 9.9 | 9.4 | 8.9 | 8.6 | 31.4 | 30.6 | 29.4 | 28.4 | 15.8 | 13.8 | 13.7 | 17.5 | 15.5 | 14.6 |
| 80 | 16.8 | 16.4 | 15.7 | 15.3 | 19.1 | 18.1 | 17.2 | 16.5 | 57.4 | 55.9 | 54.1 | 52.1 | 30.3 | 26.5 | 26.8 | 32.9 | 29.5 | 27.6 |
| Vacuum | | | | | | | | | | | | | | | | | | |
| 5 | 17.1 | 14.1 | 10.4 | 7.6 | 10.9 | 8.2 | 6.5 | 5.4 | 24.0 | 21.6 | 18.9 | 15.6 | 19.6 | 13.8 | 8.7 | 14.7 | 9.0 | 8.5 |
| 10 | 30.5 | 24.7 | 18.4 | 13.6 | 19.4 | 14.7 | 11.7 | 9.8 | 44.1 | 39.0 | 33.2 | 27.9 | 37.7 | 25.3 | 15.7 | 26.8 | 17.0 | 14.6 |
| 20 | 51.4 | 42.1 | 32.5 | 24.7 | 33.3 | 25.8 | 21.2 | 17.7 | 78.2 | 67.3 | 58.4 | 49.8 | 71.0 | 47.3 | 29.4 | 50.2 | 31.9 | 27.0 |
| 40 | 81.1 | 68.4 | 55.5 | 44.3 | 55.1 | 44.5 | 37.5 | 32.0 | 122.3 | 110.8 | 98.6 | 86.0 | 122.6 | 87.4 | 55.3 | 87.3 | 59.5 | 49.8 |

**Table 5 Maximum SEM-E frame temperature, °C**

| | Anodic rail/wedge clamp torque, N-m/lbf-in. | | | | Silver rail/wedge clamp torque, N-m/lbf-in. | | | | Nickel rail/wedge clamp torque, N-m/lbf-in. | | | | Anodic rail/bladder pressure, MPa/psig | | | Silver rail/bladder pressure, MPa/psig | | |
|---|---|---|---|---|---|---|---|---|---|---|---|---|---|---|---|---|---|---|
| Power, W | 0.56 5 | 0.90 8 | 1.24 11 | 1.58 14 | 0.56 5 | 0.90 8 | 1.24 11 | 1.58 14 | 0.56 5 | 0.90 8 | 1.24 11 | 1.58 14 | 0.689 100 | 1.034 150 | 1.378 200 | 0.689 100 | 1.034 150 | 1.378 200 |
| Air | | | | | | | | | | | | | | | | | | |
| 5 | 28.1 | 28.0 | 28.0 | 27.9 | 28.8 | 28.7 | 28.6 | 28.6 | 32.1 | 32.0 | 31.9 | 31.6 | 29.0 | 28.7 | 28.7 | 29.2 | 28.9 | 28.7 |
| 10 | 31.4 | 31.3 | 31.3 | 31.2 | 32.3 | 32.2 | 32.1 | 32.0 | 38.4 | 38.2 | 38.0 | 37.6 | 33.3 | 32.7 | 32.7 | 33.6 | 32.9 | 35.5 |
| 20 | 38.0 | 37.9 | 37.7 | 37.6 | 39.4 | 39.2 | 38.9 | 38.7 | 50.6 | 50.1 | 49.6 | 49.0 | 41.6 | 40.7 | 40.4 | 42.5 | 41.3 | 40.8 |
| 40 | 50.9 | 50.8 | 50.5 | 50.3 | 53.8 | 52.6 | 52.0 | 51.7 | 73.3 | 72.7 | 71.7 | 70.7 | 57.6 | 55.8 | 55.8 | 59.4 | 57.4 | 56.5 |
| 80 | 75.6 | 75.4 | 74.7 | 74.4 | 79.7 | 78.7 | 77.7 | 76.8 | 115.1 | 113.9 | 112.5 | 110.4 | 88.4 | 84.8 | 84.7 | 91.1 | 87.8 | 87.0 |
| Vacuum | | | | | | | | | | | | | | | | | | |
| 5 | 43.4 | 39.9 | 36.5 | 33.9 | 37.8 | 35.2 | 33.5 | 32.4 | 50.5 | 48.2 | 45.6 | 42.4 | 45.4 | 39.9 | 36.8 | 40.9 | 35.7 | 34.9 |
| 10 | 58.6 | 52.0 | 46.2 | 41.7 | 48.4 | 43.8 | 40.8 | 38.9 | 72.2 | 67.4 | 61.8 | 56.7 | 65.0 | 53.1 | 43.8 | 54.7 | 45.2 | 43.0 |
| 20 | 83.3 | 72.6 | 63.8 | 56.5 | 66.3 | 59.1 | 54.5 | 51.1 | 109.5 | 99.1 | 90.7 | 82.4 | 101.1 | 78.5 | 61.7 | 81.7 | 64.0 | 59.4 |
| 40 | 116.7 | 105.5 | 93.7 | 83.3 | 96.1 | 85.7 | 78.8 | 73.5 | 159.8 | 149.1 | 137.7 | 125.8 | 157.6 | 124.9 | 95.0 | 125.6 | 99.0 | 92.9 |

mately 25% of the conductance of the anodized SEM-E frame to the anodized card rail (anodized-to-anodized) baseline configuration. In vacuum, the anodized-to-nickel junction conductance is 50–65% of the conductance of the anodized-to-anodized baseline junction.

Although the electroless nickel plating is approximately seven times more conductive than the type II (soft) anodic coating (5 W/mK compared to 0.7 W/mK, respectively), it is five times as hard as the type II anodic coating (600 kg/mm$^2$ compared to 120 kg/mm$^2$) and is considerably rougher than the anodic coating. The substantially greater roughness of the electroless nickel plating increases the effective thickness of the gas layer in the gaps within the junction, which, in turn, increases the gas gap resistance. This is why the decrease in conductance is even more pronounced for tests in air than for tests in vacuum.

Correspondingly, the junction thermal resistance (Table 2), mean junction temperature (Table 3), junction temperature drop (Table 4), and maximum (centerline) SEM-E frame temperature (Table 5) are all greater for the anodized-to-nickel junction than for the anodized-to-anodized junction.

*2. Electroplated Silver*

Tables 1–5 provide the results of thermal tests of the silver electroplated card rail and wedge clamps. In air, the junction thermal conductance (Table 1) of the anodized SEM-E frame to the silver-plated card rail (anodized-to-silver) is approximately 85% of the conductance of the anodized-to-anodized baseline junction. In vacuum, the conductance of the anodized-to-silver junction is 135–150% of the conductance of the anodized-to-anodized baseline junction. The similar performance in air indicates that silver electroplatings would not be beneficial in this environment. However, in a vacuum environment, the 35–50% improvement in conductance afforded by silver electroplatings may substantially reduce operating temperatures and thermally induced failures.

### C. Alternative (Pneumatic Bladder) Clamps

*1. With Presently Employed Anodized Card Rail*

Thermal test results for presently used anodized (type II) card rail and alternative pneumatic bladder clamps are given in Tables 1–5. In air the junction thermal conductance increases slightly with increasing bladder pressure and heater power over the range tested. The conductance is 60% of that for the baseline combination of an anodized card rail and wedge clamp.

In vacuum, the conductance afforded by the bladder clamps is 75% of the conductance of the baseline combination (anodized card rail and wedge clamp) at the highest applied torque, 1.58 N-m (14 lbf-in.). However, the conductance at the maximum bladder pressure of 1378 kPa (200 psig) is 70% greater at low power (5 W) and 30% greater at high power (40 W) than the conductance of the baseline configuration with a specified service torque of 0.90 N-m (8 lbf-in.).

*2. With Alternative Silver Electroplated Card Rail*

Thermal test results for the silver electroplated card rail and alternative bladder clamps are given in Tables 1–5. Trends are very similar to those for the anodized card rail and bladder clamps. For tests in air the junction thermal conductance is approximately 55% of that of the anodized card rail and wedge clamp baseline combination. In vacuum the conductance of the silver-plated card rail and bladder clamps is 95% of that of the anodized card rail and wedge clamp baseline configuration.

## IV. Conclusions and Recommendations

For operation in an air environment, nickel and silver platings for the chassis card rails and bladder clamps offer no improvement in performance compared to type II anodic coatings and five-segment wedge clamps. In vacuum conditions, silver plating offers significant improvement (33–50%) in junction thermal conductance, whereas electroless nickel plating severely reduces junction conductance by 75%.

In vacuum, bladder clamps pressurized to 1378 kPa (200 psig) afford 20–70% enhancement of conductance, compared to the baseline combination of an anodized card rail and wedge clamps tightened to the specified service torque of 0.90 N-m (8 lbf-in.).

Thus, silver platings and bladder clamps may comprise a viable alternative to anodic coatings and wedge clamps for high-altitude aircraft and spacecraft. For space applications, corrosion of silver platings in the presence of monatomic oxygen in low Earth orbit is a consideration.

## Acknowledgments

Support for this investigation was provided by the U.S. Naval Surface Warfare Center in Crane, Indiana and the Center for Space Power at Texas A&M University.

## References

[1]Lambert, M. A., and Fletcher, L. S., "A Review of the Thermal Contact Conductance of Junctions with Metallic Coatings and Films," *Journal of Thermophysics and Heat Transfer*, Vol. 7, No. 4, 1993, pp. 547–554.

[2]Lambert, M. A., and Fletcher, L. S., "An Experimental Investigation of the Thermal Contact Conductance of Electroplated Silver Coatings," *Journal of Thermophysics and Heat Transfer*, Vol. 9, No. 1, 1995, pp. 79–87.

[3]Darrow, G. R., "Engineering the Sulfuric Acid Process," *Anodized Aluminum*, American Society for Testing and Materials, STP 388, Philadelphia, PA, 1965, pp. 62–84.

[4]Dini, J. W., and Johnson, H. R., "Quantitative Adhesion Data for Electroless Nickel Deposited on Various Substrates," Electroless Nickel Conf. III, Gardner Publications, Cincinnati, OH, 1983.

[5]Maclean, J. D., and Karten, S. M., "A Practical Application of Electroless Nickel Plating," *Plating*, Vol. 41, No. 11, 1954, p. 1284.

[6]Krieg, A., "Processing Procedures," *Proceedings of the Symposium on Electroless Nickel Plating*, American Society for Testing and Materials, STP 265, Philadelphia, PA, 1959, pp. 21–37.

[7]Blair, A., "Silver Plating," *Metal Finishing*, Vol. 88, No. 1A, Metals and Plastics Publications, Inc., Hackensack, NJ, 1990, pp. 268–272.

[8]Sora, V., and Bollhalder, H., "Wear Reduction of Silver-Plated Sliding Contacts," *Plating and Surface Finishing*, Vol. 75, No. 1, 1988, pp. 53–55.

[9]Kline, S. J., and McClintock, F. A., "Describing Uncertainties in Single-Sample Experiments," *Mechanical Engineering*, Vol. 75, No. 1, 1953, pp. 1–8.

[10]Lambert, M. A., Ayers, G. H., Donnelly, C. V., and Fletcher, L. S., "Thermal Contact Conductance of Electronic Modules," AIAA Paper 95-0422, Jan. 1995.